



Photocatalytic Degradation of Naphthalene by UV/ZnO: Kinetics, Influencing Factors and Mechanisms

AARAM DOKHT KHATIBI¹, KETHINENI CHANDRIKA², FERDOS KORD MOSTAFAPOUR¹,
ALI AKBAR SAJADI³ and DAVOUD BALARAK^{1*}

¹Department of Environmental Health, Health Promotion Research Center, Zahedan University of Medical Sciences, Zahedan, Iran.

²Department of Biotechnology, KoneruLakshmaiah Education Foundation, Vaddeswaram, Guntur, AP, India-52250, India.

³Student Research Committee, Zahedan University of Medical Sciences, Zahedan, Iran.

*Corresponding author E-mails: dbalarak2@gmail.com

<http://dx.doi.org/10.13005/ojc/370108>

(Received: January 12, 2021; Accepted: February 14, 2021)

ABSTRACT

Conventional wastewater treatment is not able to effectively remove Aromatic hydrocarbons such as Naphthalene, so it is important to remove the remaining antibiotics from the environment. The aim of this study was to evaluate the efficiency of UV/ZnO photocatalytic process in removing naphthalene antibiotics from aqueous solutions. This was an experimental-applied study that was performed in a batch system on a laboratory scale. The variables studied in this study include the initial pH of the solution, the dose of ZnO, reaction time and initial concentration of Naphthalene were examined. The amount of naphthalene in the samples was measured using GC. The results showed that by decreasing the pH and decreasing the initial concentration of naphthalene and increasing the contact time, the efficiency of the process was developed. However, an increase in the dose of nanoparticles to 0.8 g/L had enhance the efficiency of the process was enhanced, while increasing its amount to values higher than 0.8 g/L has been associated with a decrease in removal efficiency. The results of this study showed that the use of UV/ZnO photocatalytic process can be addressed as a well-organized method to remove naphthalene from aqueous solutions.

Keywords: UV/ZnO, Naphthalene, Photocatalytic degradation, Kinetics, Synthetic Wastewater.

INTRODUCTION

Polycyclic aromatic hydrocarbons (PAHs), are in the category of hazardous and toxic substances and have recently been identified as carcinogenic compounds¹. PAHs introduced into the water to some degree undergo physical, chemical and biological changes leading to their gradual, though

slow, degradation. They are sorbed by suspended matter, aquatic organisms and bottom sediments². Naphthalene as albobarbon, camphor tar, white tar, or naphthene, is made of two fused benzene rings and is obtained from coal^{2,3}. naphthalene is widely used for disinfection and insecticides⁴.

Pollution of water resources by naphthalene



has been reported in most industrialized countries and its permissible level in drinking water is 0.05 mg/L according to the standard of the world health organization, so its removal from industrial effluents is important^{5,6}. Among the methods of removing organic pollutants from water and wastewater, biodegradation of wastewater by microorganisms has been considered, but due to benzene rings in aromatic hydrocarbons, the biological removal efficiency is severely reduced and microorganisms are not able to break these structures^{7,8}. Therefore, in recent years, many researchers have focused on the use of modern advanced oxidation processes (AOPs)⁹. Among the various methods of this technique, the photocatalytic oxidation method using the nanophotocatalyst is a very effective method^{10,11}. This method is done by irradiating ultraviolet radiation to the surface of a semiconductor such as ZnO and TiO₂^{12,13}. These materials are excited by radiation and produce hole-electron pairs in the surface layers^{14,15}. The resulting holes have strong oxidizing properties and electron is a good reducing agent; by producing hydroxide radicals, the degradation of pollutant organic molecules occurs^{16,17}. Regarding the research on the use of nanophotocatalysts in the removal of naphthol, the following studies can be mentioned: Luo *et al.*, studied and evaluated the catalytic degradation of β -Naphthol using Degussa P25; in their study, the effect of factors, e.g., pH, concentration of the reactant and catalyst dosage was assessed¹⁸. Lee *et al.*, by hydrolysis of tetra isopropoxide (TTIP) at 100-600°C, produced TiO₂ nanoparticle and investigated the catalytic activity of this catalyst with activated carbon for degradation of β -Naphthol; the removal efficiency in this pollutant has been reported to be more than 90%¹⁹.

Although several experimental studies carried out in recent years regarding the Total pollutant removal by using nanoparticles from aquatic solution there is still a significant gap in the relevant literature with reference to the investigation adsorption capabilities of the UV/ZnO for the removal of naphthalene from aquatic solution. To the best of the authors' knowledge, there are almost no papers in the literature specifically devoted to a study of the application UV/ZnO reactor for the adsorption of naphthalene and the implementation of the design optimum process conditions in the removal naphthalene from aquatic solution.

EXPERIMENTAL

This research is an experimental study that was performed in a batch system and on a laboratory scale on synthetic solutions. Naphthalene was prepared from Merck & Co. Company. To do this, the stock solution of Naphthalene (1000 mg/L) was prepared weekly and stored in the dark at 4°C. The solutions with the desired concentrations were then prepared using the stock solution. Effect of parameters was studied in the pH values of 3, 5, 7, 9 and 11, naphthalene concentrations 5, 10, 25, 50 and 100 mg/L, the dose of zinc oxide nanoparticles in the range of 0.1, 0.2, 0.4, 0.6, 0.8 and 1 g/L, and ultraviolet lamp power (15 watts). In order to adjust the pH of the solution, 0.1 N sulfuric acid and sodium hydroxide were utilized. The experiments were performed in a 2-liter glass reactor with dimensions of 30 x 12 x 9 cm. The irradiation source was a 15 watts low-pressure UVc lamp. The lamp was inside a very transparent quartz coating with a diameter of two centimeters. The lamp was placed in the center of the container and the reactor was completely covered with aluminum foil so that the sample could be better irradiated and the radiated light would not be wasted. Inside the reactor, a magnetic stirrer was used to completely mix the sample for irradiation. To remove the nanoparticles, the samples were centrifuged at 3600 rpm for 10 minute. The remaining naphthalene in solution was measured using GC With Flame Ionization Detector (company: Agilent USA. Model: GC7890-MS5975).

Method of analysis

The concentration of naphthalene was determined by gas chromatography (GC). To inject the sample into the GC, it is necessary to transfer the sample from the aqueous phase to the organic phase. For this purpose, 10 mL of the sample was first mixed with 2 mL of dichloromethane and the mixture was put on a stirrer. After half an hour, dichloromethane, which was heavier than the aqueous sample, was separated and this process was repeated 2 more times and finally, 6 mL of naphthalene-containing dichloromethane was gently heated to bring the volume to 1 mL (it should be noted that due to the high solubility of naphthalene in dichloromethane, it remains in the organic phase and does not transfer into the gaseous phase). Finally, the temperature setting of the device was as follows: the initial temperature of the oven stays

at 65°C for one minute; the injector temperature in the splitless mode is set at 200°C, and the detector temperature is set at 210°C. Finally, after preparing the sample and adjusting the device, one microliter of the sample was injected into the device.

RESULTS AND DISCUSSION

Scanning electron microscopy (SEM) and transmitting electron microscopy (TEM) have been employed for studying the phase and crystalline structure and determining the size and shape of zinc oxide nanoparticles. Fig. 1a shows the SEM image and Fig. 1b shows the TEM image of the zinc oxide nanoparticles used in this study. The results showed that zinc oxide particles have a diameter of 50 nm and the particles used are nano in size and crystalline.

Figure 2 represents the X-ray diffraction pattern of ZnO. The diffraction peaks located at 31.84°, 34.52°, 36.33°, 47.63°, 56.71°, 62.96°, 68.13°, and 69.18° have been keenly indexed as hexagonal wurtzite phase of ZnO.

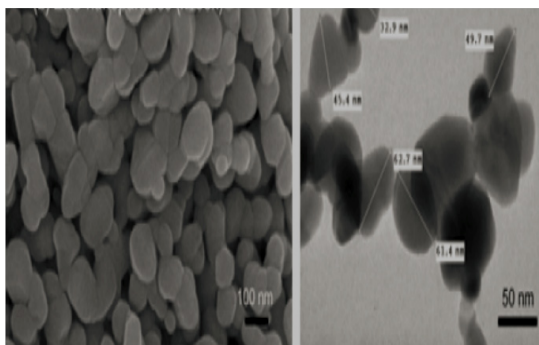


Fig. 1. micrographs of ZnO nanoparticles (a) SEM (b) TEM

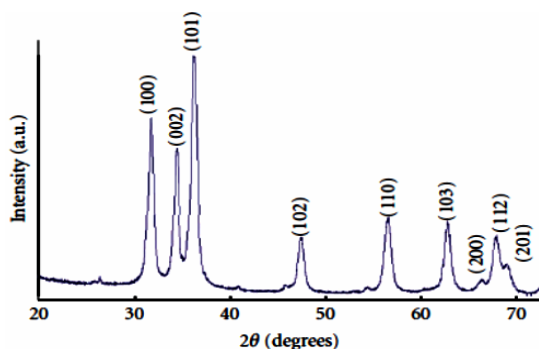


Fig. 2. XRD pattern of prepared ZnO nanoparticles
Effect of contact time

The effect of contact time was shown in Fig. 3. As can be seen in this figure, with increasing the contact time, the removal percentage of naphthalene has enhanced, so that, for example, for the power of 15 watts, the removal efficiency was reached from 53% in 10 min to 96% in 60 minute. In this study, the removal efficiency was amplified with increasing contact time. However, the removal efficiency had the highest increase in the first 10 min of the process, and over time, the increasing trend of naphthalene removal efficiency was diminished. The rapid degradation of naphthalene contaminants in the first 10 min of the process can be attributed to free radicals generated by the electron excitation of zinc oxide nanoparticles^{20,21}. Although the excitation process of zinc oxide nanoparticles and the production of hydroxyl free radicals did not decrease with increasing contact time, due to the formation of intermediate organic compounds caused by the degradation of naphthalene contaminants, some of the hydroxyl radicals produced were used to degrade these compounds^{22,23}. As a result, the removal of naphthalene contaminants is reduced. These results are consistent with the research of other researchers²⁴.

Effect of ZnO nanoparticle concentration

Figure 4 shows the effect of different concentrations of ZnO catalysts on the removal efficiency of naphthalene at pH = 3 and a concentration of 5 mg/L of naphthalene at irradiation time of 60 min for 15 watts. As can be seen in this figure, with increasing the dose of zinc oxide nanoparticles up to 0.8 g/L, the removal efficiency of naphthalene was enhanced and at higher doses, the efficiency was diminished. Initially, increasing the nanoparticle dose is led to an increase in the naphthalene removal efficiency, but the removal efficiency then decreased with increasing this amount. Therefore, the optimal value of 0.8 g/L was selected. The causes of this phenomenon are attributed to the increase in solution turbidity, reduction in UV-penetration, increase in path traveled by optical photons and decrease in the total excitable surface due to the contamination of the contaminant on the catalyst surface^{25,26}.

Effect of naphthalene concentration

As shown in Fig. 5, the removal efficiency drops with increasing naphthalene concentration. This can be explained by the fact that increasing the

concentration of naphthalene reduces the number of active sites on the catalyst surface (due to their high concentration of contaminant molecules) and thus the rate of production of oxidants such as hydroxyl free radicals due to receiving UV-rays is reduced and therefore the reaction rate is also reduced^{27,28}. As shown in the figure, at a concentration of 100 mg/L, the amount of naphthalene removal after 60 min is equal to 87%, while at a concentration of 25 mg/L, this pollutant is completely eliminated after almost 30 hours.

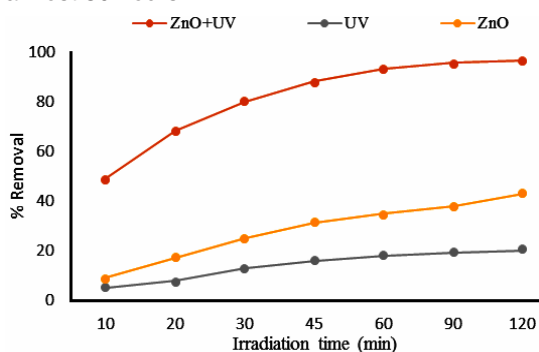


Fig. 3. Effect of contact time (pH: 7, C0: 50 ppm, Dose: 0.8 g/L)

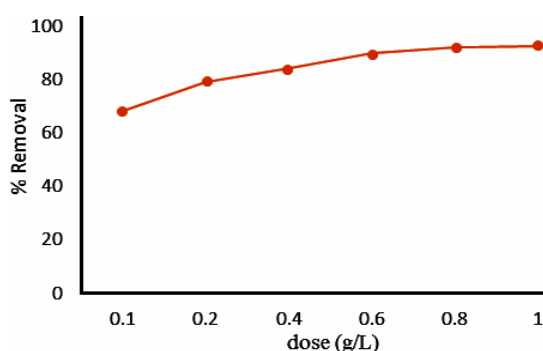


Fig. 4. Effect of ZnO dose (pH: 7, C0: 50 ppm, time: 60 min)

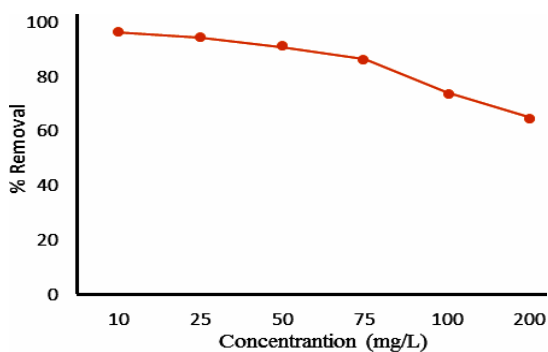


Fig. 5. Effect of concentration (pH: 7, ZnO dose: 50 ppm, time: 60 min)

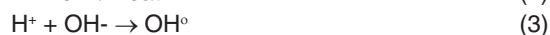
Mechanisms of photocatalytic reactions

ZnO has been used for photocatalytic

research more than any other material due to its very good properties and is one of the most active catalysts. It can be said that only TiO₂ can compete with it in terms of activity²⁹. Some of the important properties that have caused this are chemical resistance, non-toxicity, cheapness and stability. Moreover, the energy gap between its levels is 3 to 3.2 electron volts, which can be excited by light with a wavelength shorter than 385 nm. Unlike metals, which have a continuous space for moving because of free unbound electrons, semiconductors have an energy-free region, in which no energy levels are created to facilitate the recombination of the electron-hole pair created by light activation in semiconductor solids. This energy-free region, which must extend from the top of the valence band and the bottom of the conduction band (which contains the vacancies of the electrons), is called the band gap^{30,31}.

If the energy of an optical photon is equal to or greater than the band gap of a semiconductor, the absorption of this photon by the semiconductor solids will excite an electron (e⁻) from its valence band and transfer it to the conduction band. At this time, an electron vacancy or positive charge called a hole (h⁺) also occurs at the valence band. The pair of electrons and holes formed either recombine to produce heat energy or participate in redox reactions with compounds adsorbed on semiconductor surfaces. Due to the need for UV-light to perform, this catalytic role refers to that photocatalyst³².

The wavelength of 380 nm causes the electron to be excited, and the oxygen in the solution accepts the excited electron. A positively charged holes remain and produce an OH⁰ radical by adsorbing OH⁻ ions in the environment. The following reactions describe the production of hydroxyl radicals in titanium dioxide³³:



Reaction kinetics

Several factors may affect the quality of the reactions. Depending on the concentration of the

contaminant on the reaction rate, a reaction can be zero, first and second order. Based on the kinetic models of photocatalytic processes, it is determined that this process is the first order, and the Langmuir-Hinshelwood model is a kinetic model that is used to describe first order reactions at the interface between solid-liquid phases and its equation is as follows³¹:

$$R = d_c/d_t = Kr K_a C / (1 + K_a C)$$

In this regard, C, K_a, and Kr represents the initial concentration, adsorption constant and rate constant, respectively²⁸. Kr in all concentrations examined is between zero and one. In concentrations of 25, 50 and 100 mg/L is equal to 0.0272, 0.0214 and 0.0157 1/minute.

If the graph of (Ln (C₀/C_e)) against time and changes of these parameters is displayed as a straight line, the slope of the line is equivalent to a constant rate of the first-order reaction. Fig.7 shows the values of K and R² for the photocatalytic degradation reaction of naphthalene under optimal conditions. As can be seen, the trend of concentration changes with time follows a first-order kinetic model and the effect of the concentration on the rate constant of reaction can be seen (increasing the initial concentration decreases the rate constant values of reaction).

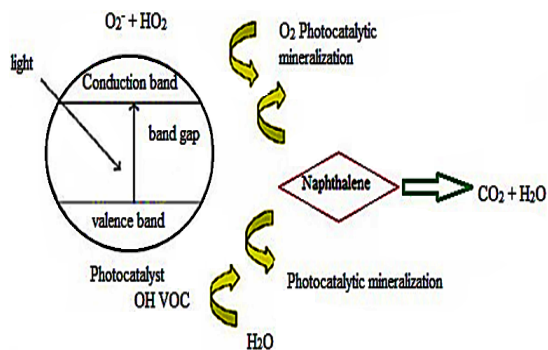


Fig. 6. Schematic of photocatalytic degradation of naphthalene

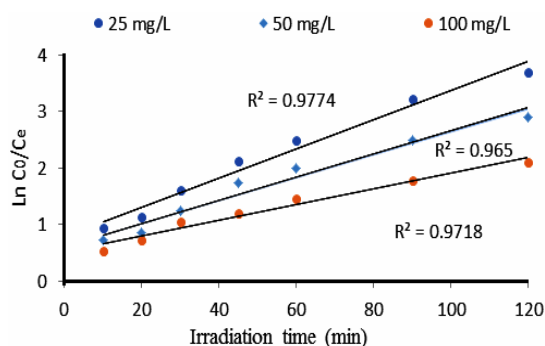


Fig. 7. Langmuir-Hinshelwood model for degradation of naphthalene

CONCLUSION

To remove non-biodegradable contaminants, instead of employing conventional biological processes, high efficient and faster photocatalytic process can be used. The percentage of naphthalene removal with a concentration of 100 ppm at pH 0.1, 0.2, 0.4, 0.6 and 0.8 after 60 min was obtained to be 76.1, 83.9, 89.2, 92.1% and 93.8 respectively. By reducing the concentration of contaminants, the removal efficiency increases so that for a concentration of 25 ppm naphthalene, the complete removal of naphthalene was acquired after 60 minute. As the concentration of ZnO nanoparticles (established on it) increases, the percentage of contaminant removal increases. The rate constants at concentrations of 25, 50, 100 ppm were equal to 0.0289, 0.0257, 0.0174; it is observed that with decreasing concentration, the reaction rate also increases.

ACKNOWLEDGMENT

The authors are grateful to the Zahedan University of Medical Sciences for the financial support of this study (Code: 9097).

Conflicting interest

There is no conflicting interest in this study.

REFERENCES

- Li, Y. H.; Di, Z. C.; Ding, J.; Wu, D. H.; Luan, Z. K.; Zhu, Y. Q. *Water. Res.*, **2005**, *39*, 605–609.
- Unlu, N.; Ersoz, M. *J. Hazard. Mater.*, **2006**, *136*, 272–280. 38. Martins, B. L.; Cruz, C. C. V.; Luna, A. S.; Henriques, A. C. *Biochem. Eng. J.*, **2006**, *27*, 310-314.
- Balarak, D.; Mahdavi, Y.; Bazrafshan, E.; Mahvi, A. H. *Fresenius. Environ. Bull.*, **2016**, *25*(5), 1321-1330.
- Meng, Y. T.; Zheng, Y. M.; Zhang, L. M.; He, J. Z. *Environ. Pollut.*, **2009**, *157*, 2577–2583.
- Pacheco, S.; Tapia, J.; Medina, M. R.; Rodriguez, R. *J. Non-Cryst. Solids.*, **2006**, *352*, 5475–5481.

6. Inbaraj, B. S.; Sulochana, N. *Ind J Chem Technol.*, **2006**, *13*, 17-23. 43. Uddin, S. M.; Azad, A. K.; Firdaus R. *Orient. J. Chem.*, **2013**, *29*(2), 241-250.
7. Malviya, A.; Kaur, D. *Orient. J. Chem.*, **2012**, *28*(2), 48-57. 45. Sirait, M.; Gea, S.; Bukit, N.; Siregar, N.; Sitorus, C. *Orient. J. Chem.*, **2018**, *34*(4), 185-191.
8. Ayuso, E. A.; Sanchez, G. *J. Hazard. Mater.*, **2007**, *147*, 594-600.
9. Diyanati, R. A.; Yousefi, Z.; Cherati, J. Y.; Balarak, D. *J. Mazandaran Univ. Med. Sci.*, **2013**, *23*, 17-23.
10. Azarpira, H.; Mahdavi, Y.; Khaleghi, O. *Pharm. Lett.*, **2016**, *8*(11), 107-113.
11. Fuhrman, H. G.; Mikkelsen, P. S.; Ledin, A. *Water. Res.*, **2007**, *41*, 591-602.
12. Balarak, D, Mostafapour, F. K.; Joghataei, A. *Pharma. Chem.* **2016**, *8*(8), 138-145.
13. Costodes, V. C. T.; Fauduet, H.; Porte, C.; Delacroix, A. *J. Hazard. Mater.*, **2003**, *103*, 121-142.
14. Ashrafi, S. D.; Rezaei, S.; Forootanfar, H.; Mahvi, A. H.; Faramarzi, M. A. *IntBiodeter. Biodegr.*, **2013**, *85*,173-181.
15. Pandey, K.; Sharma, S. K.; Sambhi, S. S. *Int. J. Environ. Sci. Tech.*, **2010**, *7*(2), 395-404.
16. Christoforidis, A. K.; Mitropoulos, A.C. *Chem. Eng. J.*, **2015**, *277*, 334 – 340.
17. Mata, Y. N.; Munoz, J. A. *J. Hazard. Mater.*, **2009**, *166*, 612-618.
18. Luo, D.; Xie, Y. F.; Tan, Z. L.; Li, X. D. *J. Environ. Biol.*, **2012**, *34*, 359 – 365.
19. Lee, S.Y.; Park, S.J.; *J. Ind. Eng. Chem.*, **2013**, *19*, 1761-1769.
20. Wei, T.; Gao S.; Wang, Q.; Xu H.; *J. Nanopart. Res.*, **2017**, *19*, 1-13.
21. Chakrabarti, S.; Dutta, B.K.; *J. Hazard. Mater. B.*, **2004**, *112*, 269-278.
22. Khan, M.M.; Adil, S.F.; Al-Mayouf, A.; *J Saudi. Chem. Soc.*, **2015**, *19*, 462-464.
23. Oturan, M.A.; Aron, A.A.; *Crit. Rev. Env. Sci. Technol.*, **2014**, *44*, 2577-2641.
24. Robertson, P.K.J.; Bahnemann D.W.; *J. Hazard. Mater.*, **2012**, *211-212*, 161-171.
25. Hermann, J.M.; *Catal. Today.*, **1999**, *53*, 115-129.
26. Riaz, U.; Asharf. S. M.; Kashyap, J.; *Mater. Res. Bull.*, **2015**, *71*, 75-90.
27. Lu, F.; Astruc, D.; *Coord. Chem. Rev.*, **2018**, *356*, 147-164.
28. Raghu, M.S.; Kumar, K.Y.; Rao, S.; Aravind, T.; Sharma, S.C.; Prashant, M.K.; Phy. B: *Condensed Matter.*, **2018**, *537*, 336-345.
29. Gallon, B.J.; Kojima, R.W.; Kaner, R.B.; Diaconescu, P.L.; *Angewanate chemie.m*, **2007**, *46*, 7251-7254.
30. Albertini, F.; Ribeiro, T.; Alvas, S.; Baleizao, C.; Farinha, J.P.S.; *Mater. Des.*, **2018**, *141*, 407-413.
31. Ghanbari, M.; Gholamrezaei, S.; Niasari, M.S.; Abbasi, A.; *J. Mater. Sci. Mater. Electron.*, **2017**, *28*, 6272-6277.
32. Yahia, I.s.; Shapaan, M.; Ismail, Y.A.M.; Aboraia, A.M.; Shaabaan, E.R.; *J. Alloy. Comp.*, **2015**, *636*, 317-322.
33. Kabirinia, F.; Mohammadreza, S.; Tabrizi, N.S.; *Powder Technol.*, **2019**, *346*, 283-290.